Received: 28 October 2022 | Revised: 17 March 2023 | Accepted: 22 March 2023

DOI: 10.1111/mec.16939

ORIGINAL ARTICLE

MOLECULAR ECOLOGY WILEY

Demographic fluctuations and selection during host–parasite co-evolution interactively increase genetic diversity

Guénolé Le Pennec[1] | Cas Retel[1] | Vienna Kowallik[2,3] | Lutz Becks[2,4] | Philine G. D. Feulner[1,5]

[1]Department of Fish Ecology and Evolution, Center for Ecology, Evolution and Biogeochemistry, EAWAG, Swiss Federal Institute of Aquatic Science and Technology, Kastanienbaum, Switzerland

[2]Community Dynamics Group, Department of Evolutionary Ecology, Max Planck Institute for Evolutionary Biology, Plön, Germany

[3]Albert-Ludwigs University Freiburg, Faculty of Environment and Natural Resources, Professorship of Forest Entomology and Protection, Stegen-Wittental, Germany

[4]Aquatic Ecology and Evolution, Limnological Institute University of Konstanz, Konstanz, Germany

[5]Division of Aquatic Ecology, Institute of Ecology and Evolution, University of Bern, Bern, Switzerland

Correspondence
Philine G. D. Feulner, Department of Fish Ecology and Evolution, Center for Ecology, Evolution and Biogeochemistry, EAWAG, Swiss Federal Institute of Aquatic Science and Technology, Kastanienbaum, Switzerland.
Email: philine.feulner@eawag.ch

Funding information
Deutsche Forschungsgemeinschaft, Grant/Award Number: BE4135/5, BE4135/9; Schweizerischer Nationalfonds zur Förderung der Wissenschaftlichen Forschung, Grant/Award Number: 310030E-160812 and 310030E_179637

Handling Editor: Wolfgang Stephan

Abstract

Host–parasite interactions can cause strong demographic fluctuations accompanied by selective sweeps of resistance/infectivity alleles. Both demographic bottlenecks and frequent sweeps are expected to reduce the amount of segregating genetic variation and therefore might constrain adaptation during co-evolution. Recent studies, however, suggest that the interaction of demographic and selective processes is a key component of co-evolutionary dynamics and may rather positively affect levels of genetic diversity available for adaptation. Here, we provide direct experimental testing of this hypothesis by disentangling the effects of demography, selection and their interaction in an experimental host–parasite system. We grew 12 populations of a unicellular, asexually reproducing algae (*Chlorella variabilis*) that experienced either growth followed by constant population sizes (three populations), demographic fluctuations (three populations), selection induced by exposure to a virus (three populations), or demographic fluctuations together with virus-induced selection (three populations). After 50 days (~50 generations), we conducted whole-genome sequencing of each algal host population. We observed more genetic diversity in populations that jointly experienced selection and demographic fluctuations than in populations where these processes were experimentally separated. In addition, in those three populations that jointly experienced selection and demographic fluctuations, experimentally measured diversity exceeds expected values of diversity that account for the cultures' population sizes. Our results suggest that eco-evolutionary feedbacks can positively affect genetic diversity and provide the necessary empirical measures to guide further improvements of theoretical models of adaptation during host–parasite co-evolution.

KEYWORDS
demography, experimental evolution, genetic diversity, host–parasite interactions, selective sweeps

Guénolé Le Pennec and Cas Retel, as well as, Lutz Becks and Philine G. D. Feulner contributed equally to this work.

1 | INTRODUCTION

Genetic diversity plays an especially important role in populations that live in fluctuating environments and undergo frequent adaptations (Barrett & Schluter, 2008; Bitter et al., 2019). Despite a long-standing interest in understanding how genetic variation is shaped in populations, it remains difficult to understand how different determinants of genetic diversity interact with each other (Buffalo, 2021; Corbett-Detig et al., 2015; Ellegren & Galtier, 2016; Leffler et al., 2012; Messer et al., 2016; Osmond & Coop, 2020). Scenarios in which evolution and ecological change occur at similar timescales complexify this question as ecology and evolution mutually affect each other (Hairston Jr et al., 2005; Hendry & Kinnison, 1999). For instance, the action of selection diminishes population size—but also allows its growth through adaptation. In return, population size changes the efficiency of selection and the supply of mutations on which selection operates (Hartl & Clark, 2007). Such feedbacks between evolutionary processes are commonplace for example in host–parasite and prey–predator co-evolution (e.g., Retel et al., 2019; Schulte et al., 2010), or in response to biocides (Antonio-Nkondjio et al., 2017; Calla et al., 2021; Waclaw, 2016). To better understand and refine predictions of how genetic diversity is shaped in populations, we need to study its variation not only over larger timescales and based on singled-out evolutionary factors, but also over short time frames where molecular, ecological and demographic factors are intertwined (Messer et al., 2016; Retel et al., 2019).

In an isolated population, genetic diversity is determined by the rate at which alleles appear by mutation and at which they disappear by selection and drift. Among others, one driver of the amount of diversity segregating in a population is its absolute size, as population size determines both the number of mutations that appear per generation (this supply is proportional to the population size) and the intensity at which variation is lost through genetic drift (Nei et al., 1975). Successions of population expansions and contractions thus affect the number of segregating sites and the distribution of allele frequencies at these sites (Tajima, 1989). Overall, large populations are expected to have higher mutation supplies and segregating variation, thus providing a larger pool of alleles that can be acted on by selection. A second important driver of genetic diversity is selection. Purifying selection removes deleterious alleles thereby lowering genome-wide diversity (Cvijović et al., 2018), but balancing selection has the opposite effect (Abdul-Rahman et al., 2021). Positive selection is the most important to consider in the context of adaptation to a novel, strong stressor. A selective sweep causes a depletion of genetic variation at and around selected variants through the hitchhiking effect (Maynard Smith & Haigh, 1974), and the depletion of genetic diversity is more severe if the local recombination rate is low (Aguadé et al., 1994; Begun & Aquadro, 1992; Charlesworth, 2020). In the absence of recombination, the complete linkage of alleles on a chromosome depletes an entire linkage group of variation, such that the hitchhiking effect of selective sweeps extends to the entire genome of clonally reproducing populations. Therefore, one general expectation is that populations that undergo frequent adaptations to new stressors and experience frequent sweeps with population size fluctuations have low genetic diversity, while populations that experience weak selective pressures and have a large size have more variation and evolutionary potential. Note, however, that in scenarios where multiple sweeping alleles compete for their expansion, their interference can slow allele fixations and maintain alleles at intermediate frequencies and thus genetic diversity (Chevin et al., 2008; Kim & Stephan, 2003; Stephan, 2019).

Strong selection is often caused by the removal of a large fraction of a population (e.g., Miller & Vincent, 2008; Zuk et al., 2006). In such scenarios, the demographic and selective histories of populations become intricately linked. A strictly gradualist perspective of evolution—where evolutionary change is slow and ecological conditions are negligible—fails to describe such scenarios and one has to consider the effect of feedbacks between ecology and evolution (Bell, 2013). In particular, environmental change can create a sequence of population size collapse, selective sweeps and population regrowth. Genetic diversity is likely to be affected in a complex fashion by such successions, with demographic fluctuations modulating the mutation supply and genetic drift, as well as the intensity and direction of multiple density-dependent selection pressures. Incorporating such feedbacks between evolution and population sizes is necessary to understand the dynamics of genetic diversity during rapid evolution (Messer et al., 2016). While we can make progress by producing more complex population genetics models that incorporate eco-evolutionary feedbacks, these models need to be motivated and compared to empirical results (Buckingham & Ashby, 2022).

Co-evolution of microbial hosts with a parasitic virus can give rise to fast-paced evolution and is ideal to study co-evolution in laboratory conditions (Brockhurst et al., 2007; Frickel et al., 2016; Mizoguchi et al., 2003; Retel et al., 2019). In particular, arms-race dynamics, where hosts and parasites evolve in response to each other, is characterized by frequent sweeps and population size fluctuations (Buckling & Brockhurst, 2012). Resistance (i.e., the ability of a host to maintain high fitness in presence of the parasite) can evolve as a mechanism that prevents attachment, penetration or virus replication inside the cell, as well as by blocking cellular lysis or evolving a tolerance to infection (Stern & Sorek, 2011). In the laboratory, any segregating or de novo mutations conferring resistance to the host can rapidly sweep and restore positive population growth in the presence of the virus and allow us to study interactions between demography and selection experimentally. It is already known that interactions of demographic fluctuations with selection have wide-reaching consequences in host–parasite co-evolution (Hesse & Buckling, 2016; Ashby et al., 2019), including changing temporal dynamics (de Andreazzi et al., 2018; van Velzen & Gaedke, 2017, 2018), the balance of stochasticity and determinism of evolutionary trajectories (Gokhale et al., 2013), and the conditions under which diversity persists (Ashby et al., 2019). However, it is not known to what extent demography–selection interactions shape host genetic diversity (but see Retel et al., 2019). As genetic diversity is essential to host persistence (Ekroth et al., 2019), empirical measures of

the effect of interactions on genetic diversity are required to understand host–parasite dynamics and provide fundaments for theoretical models.

We present results of a 60-day co-evolution experiment in a microbial host–parasite system. Our experimental setup aims to measure the separate and joint effects of demographic fluctuations and of selection induced by parasitism on the hosts' genetic diversity. We grew microalgae *Chlorella variabilis* (strain NC64A) in a flow-through system that allows manipulation of the population size by adjusting the substrate's dilution rate. To measure the effect of selection induced by the virus and demographic fluctuations together, we inoculated some cultures with Chloroviruses (*DMS*; see Section 2). These cultures were previously studied in Retel et al. (2019). In separate cultures, we measured the effect of demographic fluctuations alone by growing the algae without virus but inducing demographic fluctuations through adjusting dilution rates of the flow-through system at certain time points (*DEM*). To measure the effect of selection alone, we grew algae with virus in an environment with a constant but increased dilution rate to minimize demographic fluctuations (*SEL*). We hypothesized that demographic fluctuations negatively affect genetic diversity such that the control treatment (*CON*) free of virus-induced selection and of demographic fluctuations would have the highest levels of diversity. Second, we hypothesized that the presence of virus negatively affected genetic diversity because of the depleting effect of resistance alleles sweeping in the host population (Frickel et al., 2016). Third, we hypothesize that the joint effect of demographic fluctuations and selective sweeps is not an addition of individual effects but that these two factors interact, as suggested in Retel et al. (2019). Our experimental measures provide direct evidence for the role of feedbacks between selection and demography, and show that this interaction retained or accelerated the replenishment of genetic diversity of the algae hosts during co-evolution.

2 | MATERIALS AND METHODS

2.1 | Overview of the experiment

To study a host–parasite system, we used the unicellular green algae *Chlorella variabilis* strain NC64A and the lytic virus *Paramecium bursaria* chlorella virus-1 (PBCV-1). In nature, *Chlorella variabilis* NC64A is a natural endosymbiont of the ciliate *Paramecium bursaria*, but it can also be grown in the laboratory in free-living conditions. The algae's generation time is ~24 h under standard laboratory conditions and it has a genome size of 46.2 Mb. The *Chlorovirus* virus PBCV-1 is a large double-stranded DNA virus. *Chloroviruses* infect *Chlorella*-like green algae (Agarkova et al., 2014). Both the algae and the virus are haploid and reproduce asexually. We conducted the experiment using continuous flow-through systems (chemostats) as previously described (Frickel et al., 2016; Retel et al., 2019). Chemostats were continuously supplied with a modified version of Bold's Basal Medium (BBM), mixed by stirring, and maintained at 20°C with constant light.

To study the separate and combined effects of strong selection and demographic fluctuations, we applied treatments in a factorial design with four treatments and three replicate cultures per treatment, producing a total of 12 cultures. The experimental cultures grew for 60 days. At the beginning of the experiment, we inoculated all 12 chemostats with a common *Chlorella* stock culture derived from a single algal clone. With this initial inoculation from one isogenic ancestor, we aimed to minimize the initial genetic differences between chemostats. After 12 days, we inoculated isogenic PBCV1 virus in half (six) of the cultures. These six cultures are part of two treatments with virus-induced selection. In three cultures with virus, we maintained a constant flow-through rate of 0.1 of the volume per day. Since we expected selection and demographic variation to occur together in this treatment, we refer to these cultures as treatment *DMS* (for DeMography and Selection). The cultures of the *DMS* treatment have been analysed previously in Retel et al. (2019). In the remaining three cultures with virus, we increased the daily dilution rate to 0.3 from day 12 until the end of the experiment. Changes in dilution rates have previously been shown to change the dynamic behaviour of populations (between a cyclical and a steady state in population sizes) and in cycle amplitudes (e.g., Becks & Arndt, 2013) such that we expected the increased dilution rate of the chemostats to reduce the amplitude of the demographic changes, thereby minimizing the effect of population size fluctuations in this treatment. We refer to these cultures as treatment *SEL* (for SELection). In three cultures without virus, we replicated the demographic history of the treatment *DMS*, thereby isolating the effect of demography from the effect of virus-induced selection (cultures hereafter called treatment *DEM*, for DEMography). To produce demographic fluctuations, we modified the dilution rate of these three cultures simultaneously between 0 and 1.2 per day over time. Finally, three control cultures of algae were grown in the absence of virus under a constant flow-through rate of 0.1 of the volume per day (treatment *CON*, for CONtrol), as previously presented in Retel et al. (2019).

2.2 | Population size measurements

We measured population sizes of the algae and of the virus each day. Algae samples were fixed with 2.5% Lugol for later quantification using imaging flow cytometry (FlowCam, Fluid Imaging Technologies) using the protocol described in Retel et al. (2019). In the plots, log-transformed population sizes of both species were smoothed with cubic splines with the *smooth.spline* function in R (R Core Team, 2022). To provide a statistic representing the overall population sizes of each culture throughout the experiment, we calculated the harmonic means of the daily population sizes between day 2 and the day of sampling (54 [control cultures] and 51 [cultures of other treatments]). Harmonic means of population sizes *N* can be

used as approximations of the effective population size N_e when N fluctuates (Rice, 2004).

2.3 | Analysis of resistance and growth rates

To study how the presence and absence of virus affected phenotypic evolution in host populations, we collected and preserved algae and virus samples at regular intervals to perform time shift experiments (for details see Frickel et al., 2016). We measured the resistance of the algae as the experiment progresses against an array of viruses sampled throughout the experiment. For this, we selected nine (treatments *SEL* and *DMS*) and three (treatments *CON* and *DEM*) time points and conducted infection assays. We sampled more points for the treatments with virus, as we aimed to follow the evolution of resistance and we did not expect evolution of resistance in the treatments without virus based on previous experiments with this system (Frickel et al., 2016). For each of the time points, a subset of 10–12 algal clones per time point were regrown individually in liquid BBM. We then exposed clonal populations of each isolated host individually to virus population from the nine selected time points (including the ancestral virus) with an initial ratio of algal cells to virus particles of 0.01 in 200 μL in 96-well plates and we tracked algal growth for 3 days. Algal growth rates were calculated from optical density measurements (Infinite M200PRO; Tecan) taken at $t = 0$ and $t = 72$ h. For each combination of algal clone and virus population, we conducted four technical replicates. Algal clones were said to be resistant to a virus population when the mean growth rate ± 2 *SD* of the technical replicates per clones in wells containing virus and in wells without virus overlapped (Frickel et al., 2016). From these tests, we calculated a resistance range for each host clone as the proportion of virus populations to which the host is resistant (range 0–1). For clones coming from the treatments *CON* and *DEM*, we performed resistance assays with ancestral virus only.

To explore whether resistance evolved at different speeds in the treatments that received virus, *SEL* and *DMS*, we analysed changes in the clones' resistance ranges over time, between the date where virus was inoculated (day 12) until the end of the experiment (day 60). This includes eight time points per treatment and 10–12 clones per time point per treatment. We performed a regression on a linear mixed model, regressing the *resistance ranges* of individual clones over *time* (in days), *treatment* (*SEL* or *DMS*), and the interaction between *time* and *treatment*. We also added a variable of random effect, *batch* (from one to 12), with a random intercept and fixed slope. We used this random effect to account for the nonindependency of clones coming from one chemostat. We used a likelihood ratio test comparing the above model with a model where the interaction between *time* and *treatment* was removed. The speed at which resistance evolved would be considered different between treatments *SEL* and *DMS* if the likelihood ratio test between both models was significant at a threshold $p < .05$. Linear mixed models were built with the function *lmer* of the R package LME4 (version 1.1.29; Bates et al., 2015) and likelihood ratio test performed with the function *anova* of the R package STATS (version 1.1.29).

To test whether growth rates of the host evolved during the duration of the experiment, we compared the slopes of linear regressions of growth rate against time (through the entire duration of the experiment) with null models. To do this, we considered the 10–12 algal clones sampled at six time points for the treatments that did not receive virus (*CON* and *DEM*) and at nine time points for the treatment with virus (*SEL* and *DMS*). To provide for measures of growth in an equivalent, nonstressing environment, we considered growth rates of these clones in the absence of virus. For each of the four treatments, we built a linear mixed model with the *mean growth rate* as the dependent variable, *time* (in days) as the independent variable and *batch* (from 1 to 12) as a random effect with fixed slope to account for different mean growths between replicates. The model was build using the function *lmer* of the package LME4 (version 1.1.29). We performed a likelihood ratio test with the function *anova* of the package STATS (version 1.1.29) to assess whether *time* had an effect on the *mean growth rate* of the clones. We realized this test by comparing the likelihood of the full model against a model where the time variable was removed. We calculated values of R^2 for mixed models with the function *r.squarredGLMM* of the R package MUMIN (version 1.46.0; Bartoń, 2022).

2.4 | Analysis of genetic data

To test for the effects of selection by the virus, demographic bottlenecks and the interaction of the combined factors on genetic diversity (nucleotide diversity and segregating sites), we selected time points where cultures with virus had undergone multiple rounds of growth and reduction in population size and multiple incremental steps in the host resistance range. After day 50, algae in the treatment *DMS* had undergone at least two sweeps for resistance (Retel et al., 2019). We selected day 51 for the treatment *DEM*, *SEL* and *DMS* and day 54 for the control treatment *CON* (day 54 was the first day sampled after day 50 for that treatment). On these dates, we sampled 40 mL of liquid from each chemostat and centrifuged them at ~35,000*g* for 2 h to obtain pellets. We froze the pellets at −80°C for later DNA extractions. To extract DNA, we used DNeasy Blood and Tissue kits with minor modifications. We started by incubating 100 μL of buffer ATL, 30 μL of proteinase and 200 μL of concentrated sample at 56°C for 4 h, then adding 600 μL of 1:1 buffer AL + ethanol mix and subsequently followed the standard column-based protocol (elution in 50 μL elution buffer).

For sequencing, we prepared libraries with Illumina NexteraXT kits and conducted paired-end 150-bp sequencing. Populations from the treatment *DMS* were sequenced on four runs of an Illumina NextSeq machine (Max Planck Institute for Evolutionary Biology) and are a subset of the data published in Retel et al. (2019). We sequenced the other nine populations on two lanes of an Illumina NovaSeq S1 (NGS platform at Bern University). We included a sample from a clonal population of the ancestral host in both

the NextSeq and NovaSeq sequencing batches. We performed preprocessing of the sequencers' output reads with FASTP (Chen et al., 2018). This consisted of trimming Illumina adapter sequences and polyG tails (default settings), and merging forward and reverse reads in case they overlapped (with the settings *overlap_len_require* to 20, *overlap_diff_limit* to 5 and *overlap_diff_percent_limit* to 5). We also trimmed 3′ end tails of reads if the mean quality dropped below 15 and removed reads shorter than 70 bases. Reads were aligned on the *Chlorella variabilis* reference genome (Blanc et al., 2010) with BWA MEM version 0.7.17 (Li & Durbin, 2009) using default parameter settings. We ran SAMTOOLS version 1.9 (Li et al., 2009) fixmate and PICARD version 2.0.1 (http://broadinstitute.github.io/picard) AddOrReplaceReadGroups to create unique read groups per library per sequencing batch per lane. We then merged the resulting alignment files per sample (SAMTOOLS *merge*), sorted the resulting bam files (PICARD *SortSam*), removed duplicate reads (SAMTOOLS *markdup*), and cleaned (PICARD *CleanSam*) and indexed (SAMTOOLS *index*) the files. We created a pileup file with the SAMTOOLS *mpileup* function. To minimize the quantity of base call and mapping errors, we used stringent quality filtering on the variation retained in this variant file by removing bases with a quality <35 and alignments with a score < 35. We removed indels of the pileup file with the parameter *skip-indels* in SAMTOOLS *mpileup*.

To allow comparison of genetic diversity between samples with different depth of coverage, we standardized all files to a uniform coverage of 6× using the function *subsample-pileup.pl* of the software POPOOLATION version 1.2.2 (Kofler et al., 2011). We fixed this depth of coverage to retain a maximum of 1-kb genomic windows with sufficient coverage to calculate genetic statistics in the 12 samples. We then used POPOOLATION's function *variance-sliding.pl* to calculate nucleotide diversity (π), segregating sites, and Tajima's *D* for nonoverlapping 1-kb windows. We only included windows that were fully covered with 6× depth by setting the *variance-sliding.pl* options as follows: *--pool-size* 1000 *--min-count* 1 *--min-covered-fraction* 1. To assess the number of segregating sites in all samples, we used the output log of *variance-sliding.pl* to extract the number of variable sites used in the calculation of nucleotide diversity with a custom bash script.

To be able to compare empirical measures with theoretical expectations, we calculated the expected nucleotide diversity (π_{exp}) and segregating sites (S_{exp}) in populations at statistical equilibrium. The expected nucleotide diversity in *Chlorella* populations at mutation–drift equilibrium was obtained with the formula $\pi_{exp} = 2N_e\mu$ (Hartl & Clark, 2007). The value N_e was approximated as harmonic means of population sizes (see Section 2.2) and μ the mutation rate. Since mutation rates in *Chlorella variabilis* are not known, we presented results for a range of three plausible mutation rates: 10^{-9}, 10^{-10} and 10^{-11}. The expected number of segregating sites when sampling *i* sequences in the population was calculated with equation 1.4a of Watterson (1975) as follows: $S_{exp,i} = 2N_e\mu \sum_{j=1}^{i-1} 1/j$. We used $i = 6$ as all positions in the observed genetic data were subsampled to a uniform 6× depth of coverage.

To understand the effect of selection and demography on the genetic nucleotide diversity in *Chlorella* cultures, we used the R package LME4 (version 1.1.29) for mixed modelling to construct the following linear mixed model: $\log(\pi_{ij} + 1) = \beta_0 + \beta_1 \text{demography}_i + \beta_2 \text{selection}_i + \beta_3 \text{interaction}_i + \beta_{0i} + \varepsilon_{ij}$. To use a linear regression on the right-skewed data of genetic diversity, we performed a $\log(x+1)$ transformation of the genetic diversity variable (Kirchner, 2020). Given that π can be equal to 0, the +1 allows taking the logarithm of the data set while retaining the property of the log transformation. The model has the log +1 of observed nucleotide diversity (π_{obs}) as the dependent variable, and three independent variables of fixed effect (*selection*, *demography* and the *interaction* between the two) and one variable of random effect (*batch*). The variable *selection* is a vector of 0 and 1 corresponding to the presence or absence of virus in a culture. The variable *demography* is equal to 1 minus the (log of) harmonic mean of a given culture's population sizes (N_e) divided by the (log of) average N_e in the control treatment ($1 - \log(N_e \text{ of a culture})/\log(N_e \text{ of controls})$). Thus, *demography* is higher in populations that have experienced overall lower population size. The variable *interaction* is the interaction between the variables *selection* and *demography* as encoded in the model by the syntax *demography: selection* in R. The variable *batch* captures the random effect caused by the growth of independent replicate populations per treatment by fitting a different intercept for each culture. To analyse a data set with a balanced number of observations between treatments, we reduced the data set to create a table with an equal number of observations per treatment. *DMS* was the treatment with the fewest genomic windows (923) with full 6× coverage. We balanced the number of observations by sampling 923 genomic windows in each of the treatments *CON*, *DEM* and *SEL* and keeping the 923 genomic windows for *DMS*. We verified that the results of the statistical tests remained consistent when sampling different genomic windows. We tested statistical significance of the predictor variables on genetic diversity with a type 3 ANOVA test using the function *anova* of the package STATS. We fitted a comparable model with observed segregating sites S_{obs} as the dependent variable (without log +1 transformation), to the variables *demography*, *selection*, *interaction* and *batch* as described above. The model's family was set to be a Poisson distribution to fit count data. To be able to use a Poisson distribution, we used the function *glmer* of the R package LME4 and specified the option *family = poisson*. To provide for a balanced number of observations per treatment in the ANOVA, we used the same subsampled data set as above. To test the significance of individual variables, we conducted an ANOVA comparing the full glm model against models where single variables were alternatively removed and performed likelihood ratio tests with the function *anova* of the package STATS. To estimate values of R^2 for the above mixed models, we used the function *r.squarredGLMM* of the R package MUMIN (version 1.46.0; Bartoń, 2022). In the case of the segregating sites model that assumed a Poisson distribution, we reported the R^2 estimated from the lognormal distribution

(Nakagawa et al., 2017). We report *p*-values corrected with the Benjamini–Hochberg method using the R function *p.adjust* (package STATS version 3.6.2).

3 | RESULTS

3.1 | Population size variation

We present the result of an experiment that aimed to disentangle the effects of demographic fluctuations, of selection exerted by a virus, and of the interactions of fluctuations and selection on the genetic diversity of an algae host. In treatment *CON*, the host populations grew steadily to reach a maximum population size of ~7×10^8 cells about 30 days after the start of the experiment (Figure 1). In the treatment *DMS*, the presence of the virus resulted in large fluctuations of host population sizes of about two orders of magnitude and population size variations of the three replicates were highly consistent (more information in Frickel et al., 2018; Retel et al., 2019). Population size changes in the treatment *DEM* followed experimental manipulations of the dilution rates. Although these did not precisely match variations in the treatment *DMS*, the harmonic means of population sizes in the treatment *DEM* are close to that of the treatment *DMS*. In the treatment *SEL*, where we aimed to reduce demographic fluctuations by increasing dilution rates, some demographic fluctuations remained but amplitudes were reduced at one order of magnitude compared to the treatments *DMS* and *DEM*. The harmonic means of population size were highly consistent within treatments, with *CON* ($10^{8.58 \pm 0.05}$) and *SEL* ($10^{7.97 \pm 0.9}$) treatments having the highest population sizes overall, and *DEM* ($10^{7.59 \pm 0.03}$) and *DMS* ($10^{7.46 \pm 0.05}$) treatments the lowest, as intended by our experimental setup. To compare the relative magnitude of bottlenecks that occurred in each treatment we calculated minimum-to-maximum population size ratios. From day 12 (introduction of virus) until day 54, the ratio between minimum and maximum population sizes measured in treatment *CON* was 1/2.47. In contrast, in treatment *DMS*, bottlenecks induced by the virus led to a strong population size reduction by a factor of 1/250. In treatment *DEM*, the bottlenecks led to a reduction by a factor of 1/26 and in treatment *SEL*, bottlenecks were reduced by a factor of 1/8.8. This demonstrates that increased dilution rates considerably lowered demographic fluctuations in treatment *SEL* relative to treatment *DMS*.

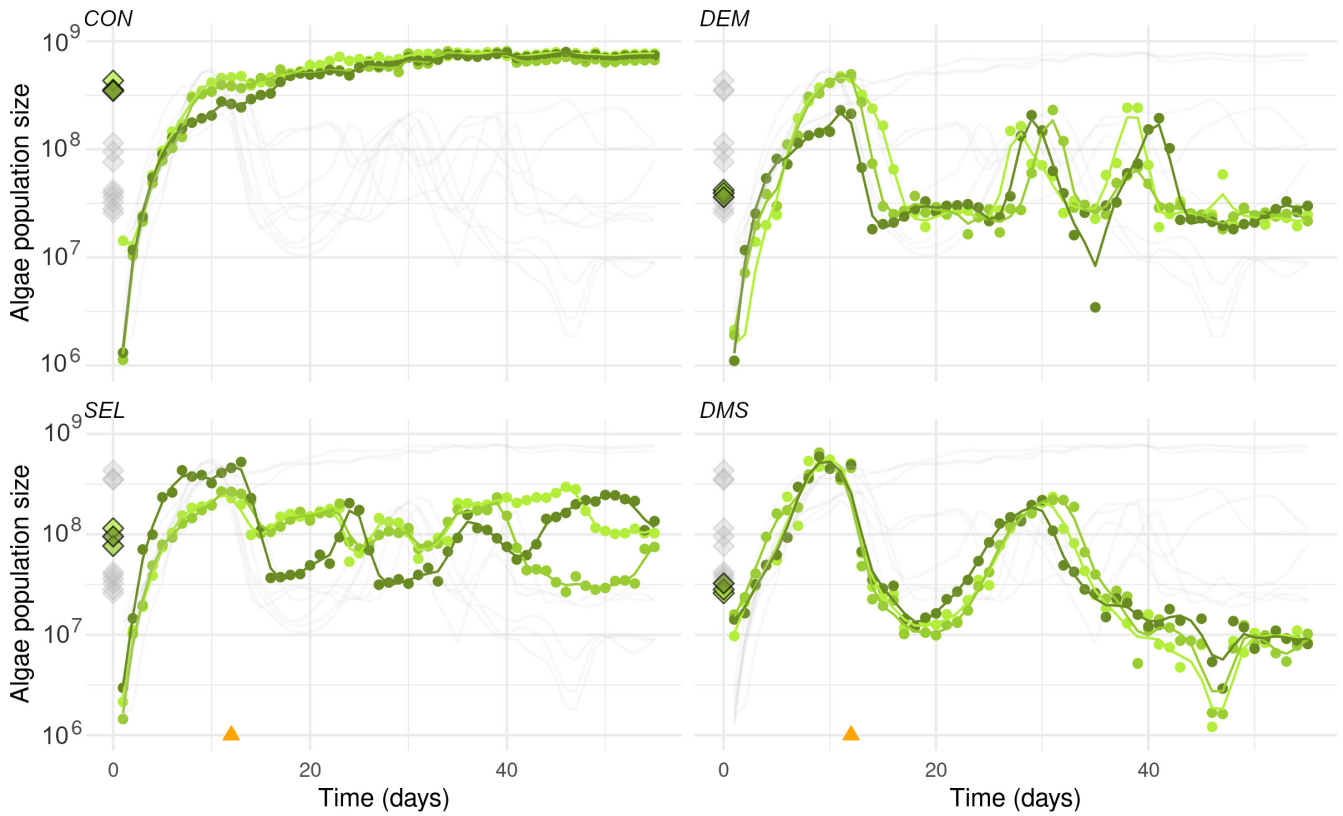

FIGURE 1 Population sizes of algae in the four treatments. Green dots are daily measures of the number of algae cells, as cells on a $\log_{10}$-scale. Different shades of green mark the three replicates of each treatment. To facilitate comparisons between treatments, measures of all experimental populations are plotted in light grey. The harmonic means of population sizes are represented as diamonds on the left of each plot. All populations were inoculated with *Chlorella* algae from the same clonal population. The time point of introduction of PBCV-1 virus (for *SEL* and *DMS*) is marked with an orange triangle. The control treatment (*CON*) had a constant dilution rate (0.1) in the absence of virus. The demographic treatment (*DEM*) had a variable dilution rate leading to population size fluctuations. The selection treatment (*SEL*) had virus and an increased dilution rate (0.3) to reduce population size fluctuations. The demography-and-selection treatment (*DMS*) had virus and a constant dilution rate (0.1).

3.2 | Evolution of resistance and growth rate

In the treatment *CON* where no demographic fluctuations occurred, all but one of 180 (60 per replicate) tested clones were susceptible to infection by the ancestral PBCV-1 viruses (Figure 2a). In the treatment with demographic fluctuations (*DEM*) we found 11 clones among the 180 clones tested per replicate to be resistant to ancestral virus. In all cultures that received virus (treatments *SEL* and *DMS*) the host's resistance range increased with time. In particular, resistance evolved at least three times (in response to the evolution of novel infectious virus strains in the populations, vertical lines in Figure 1a) in the *SEL and DMS* treatment, following a pattern of arms-race dynamics. We found statistical evidence for the effect of demography on resistance evolution comparing treatment *SEL* vs. *DMS* ($\chi^2(1)=10.093$, $p=.0015$). Host populations that experienced selection through the virus therefore evolved resistance at a faster rate in the treatment with weak demographic fluctuations (*SEL*) compared to the treatment with large demographic fluctuations (*DMS*). After addition of the virus, resistance evolved 16% faster in the algae in treatment *SEL* than in treatment *DMS*.

We tested whether the growth rate of the host evolved throughout the experiment and if the speed of this evolution depended on the treatments. Likelihood ratio tests on linear mixed models revealed a significant change in host growth rates in treatment *CON* ($\chi^2(1)=7.482$, $p=.018$) and *SEL* ($\chi^2(1)=53.76$, $p<.001$), but no significant changes were found in treatment *DEM* ($\chi^2(1)=0.644$, $p=.422$) or *DMS* ($\chi^2(1)=3.854$, $p=.099$). Despite *CON* and *SEL* both having a significant association of time with growth rate, in the treatment *SEL* the *time* variable captures $R^2=13\%$ of the growth rate variation, while only $R^2=3\%$ of the growth rate variation in treatment *CON* is captured by the *time* variable (Figure 2b).

3.3 | Interaction of demography with selection

To test how the host's genetic diversity was affected by demography, selection and both processes together, we sequenced cultures of *Chlorella* at day 51 (except treatment *CON*, sampled at day 54) after the start of the experiment. Treatment *CON*, where populations grew without virus-induced selection and without demographic fluctuations, had the highest genome-wide estimates of nucleotide diversity. The treatment with demography alone (*DEM*) caused the largest genetic diversity reduction relative to the values obtained in control populations (Figure 3a). Interestingly, the combination of demographic fluctuation and selection in treatment *DMS* produced cultures with a higher genetic diversity than treatments with viral selection (*SEL*) or demographic fluctuations (*DEM*). To assess whether different population sizes were sufficient to explain the higher diversity in *DMS* compared to *DEM* and *SEL*, we calculated the expected nucleotide diversity $\pi_{exp}=2N_e\mu$ of theoretical populations at mutation–drift equilibrium with an effective population size N_e taken to be the harmonic mean as measured in the 12 experimental populations and for three different hypothetical values of mutation rate μ. Results show that observed nucleotide diversity π_{obs} of cultures in treatments *CON*, *SEL* and *DEM* were lower than π_{exp} calculated with a mutation rate of $\mu=10^{-11}$ using the population size measured in each culture. In contrast, nucleotide diversity π_{obs} of the three cultures of the treatment *DMS* was intermediate between values of π_{exp} calculated with a mutation rate $\mu=10^{-11}$ and $\mu=10^{-10}$ (Figure 3b).

We found segregating sites to follow the same trend as nucleotide diversity in all cultures, with treatment *CON* having the highest average density of segregating sites followed by *DMS*, *SEL* and *DEM* (Figure 3c). To assess whether population size differences could explain the distribution of segregating sites across cultures, we compared the observed density of segregating sites, S_{obs}, with a theoretical estimate of a population at mutation–drift equilibrium $S_{exp}=2N_e\mu\sum_{j=1}^{5}1/j$. With the exception of cultures of treatment *DMS*, we found segregating site values S_{obs} to lie between S_{exp} calculated with mutation rates $\mu=10^{-9}$ and $\mu=10^{-10}$. In contrast, the three cultures in treatment *DMS* had a density of segregating sites above S_{exp} calculated with $\mu=10^{-9}$ (Figure 3d).

From comparisons of theoretical equilibria and measured values, we found that empirical values of segregating sites suggest a much higher mutation rate than nucleotide diversities (Figure 3b,d), which indicates an excess of rare alleles compared to a mutation–drift equilibrium. Tajima's *D* is a combination of nucleotide diversity and the number of segregating sites, with negative values corresponding to an excess of rare alleles relative to an expected equilibrium value. Accordingly, we found all populations to have, on average, negative values of Tajima's *D* across genomic windows (Figure 3e). This negative Tajima's *D* reflects a population expansion or a recent selective sweep, which is congruent with the demographic history of the experimental populations.

The factorial design of the experiment allowed us to quantify the effects of demography, selection and their interaction on genetic diversity in the algae host populations. For this, we used a mixed model with observed nucleotide diversity $\log(\pi_{obs}+1)$ as the dependent variable, two independent variables of fixed effects *selection* and *demography*, and one variable of random effect *batch* that captured variation between replicate cultures. The variable *selection* was a vector of zeros and ones matching to the presence of virus in a culture. The variable *demography* reflected the magnitude of population size bottlenecks, with *demography* approaching 0 when population size was similar to that of control populations and approaching 1 if population sizes were very small. Results of the fitted parameters are provided in Table S1. The fixed effects fitted in this model explained $R^2=.43$ of the variance in nucleotide diversity (conditional $R^2=.60$ including fits of random effects). Performing an ANOVA on this model showed that *demography* has a statistically significant effect on nucleotide diversity ($\chi^2(1)=17.067$, $p<.001$), and that *selection* has a statistically significant effect on nucleotide diversity ($\chi^2(1)=6.834$, $p=.009$). Furthermore, the two-way ANOVA revealed a statistically significant interaction between the variables *selection* and *demography* ($\chi^2(1)=8.723$, $p=.006$). In the model with all variables, the sign of the fitted coefficient was negative for the variables

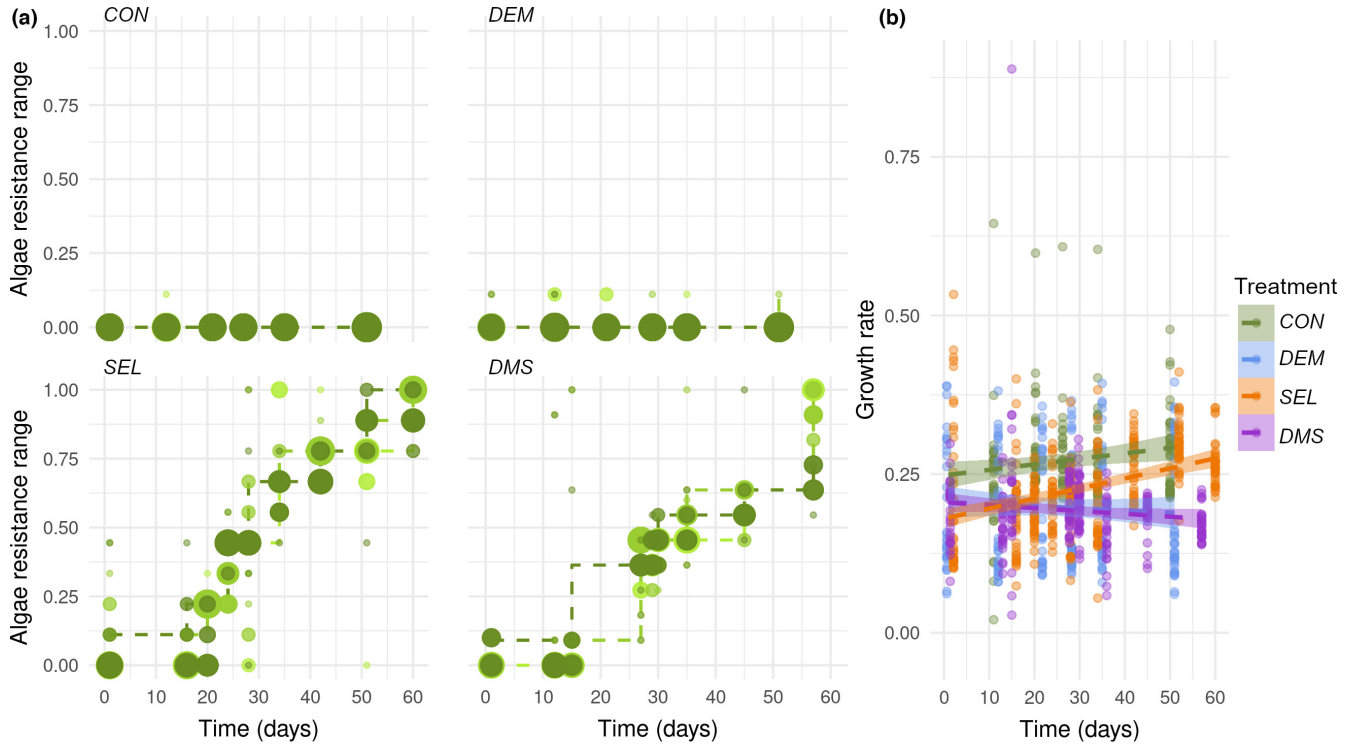

FIGURE 2 Phenotypic evolution in the algae host. (a) Resistance range against time (in days) for each of the treatments produced in the study. The growth of 10–12 algae clones in the presence of virus was measured to test for resistance. An algae resistance range of 0 (resp. 1) implies that the algae is resistance to none (resp. all) of the viruses used in the assays. The size of the dot is proportional to the number of algal clones with the same resistance range. Dashed lines show the highest resistance ranges maintained by at least two clones at all consecutive time points. The three replicates per treatment are coloured with different greens. (b) Average growth rate of *Chlorella* clones in the absence of virus. For each sampled time point, we grew 10–12 clones in the absence of virus and used the average growth rate of four technical replicates. Lines show the regression of average growth rates against time for each treatment. Statistical analysis reveals a significant evolution of host growth rates in treatments *CON* and *SEL*.

selection (−0.002 ± 0.001 [*SE*]) and *demography* (−0.014 ± 0.003) and positive for the *interaction* (0.019 ± 0.006).

To test the effects of *demography*, *selection* and their interaction on the density of segregating sites, we constructed a generalized linear model fitting a Poisson distribution. The fixed effects of *selection*, *demography* and their interaction explained $R^2 = .62$ of the variance in the density of segregating sites (conditional $R^2 = .68$ with random effects). Comparison of the full model with models that excluded a single variable through a likelihood ratio test showed that *demography* had a statistically significant effect on segregating sites ($\chi^2(1) = 28.644$, $p < .001$), as well as the presence of *selection* ($\chi^2(1) = 10.607$, $p = .001$). The two-way ANOVA detected a statistically significant interaction between *selection* and *demography* affecting the density of segregating sites ($\chi^2(1) = 10.208$, $p < .001$). In the full model, the sign of the coefficient was negative for the variables *selection* (−1.672 ± 0.324 [*SE*]) and *demography* (−18.773 ± 1.643) and positive for the *interaction* (26.086 ± 3.247).

4 | DISCUSSION

We performed experimental manipulations on populations of an algae host and measured the effects of selection, demographic fluctuations and their interaction on algal genetic diversity. All algal populations were started from the same source population that was grown from one clone. Each of the four different treatments was replicated three times with combinations of presence/absence of selection exerted by a lytic virus and demographic fluctuation. These treatments include a control treatment (*CON*) with constant host growth in the absence of virus, a demographic treatment (*DEM*) where host population size varied through manual adjustments of the cultures' dilution rates, a selection treatment (*SEL*) with virus and reduced population size fluctuations through increased dilution rate (0.3), and a demography-and-selection treatment (*DMS*) with virus and constant dilution. We used a pooled sequencing approach on the populations to quantify the effects of virus-induced selection, demographic fluctuations and their interaction on the genetic diversity of hosts. Previous work has demonstrated that genomic variation in the virus population is restricted to the same few genes in both treatments (Retel et al., 2022).

Previous experiments using *Chlorella* and PBCV-1 found highly repeatable evolution with respect to the timing and magnitude of population size variations as well as host resistance and virus host ranges (Frickel et al., 2016, 2018). Co-evolution between host and viruses in treatment *DMS* likewise produced large population size variation that was highly repeatable across replicates (discussed in

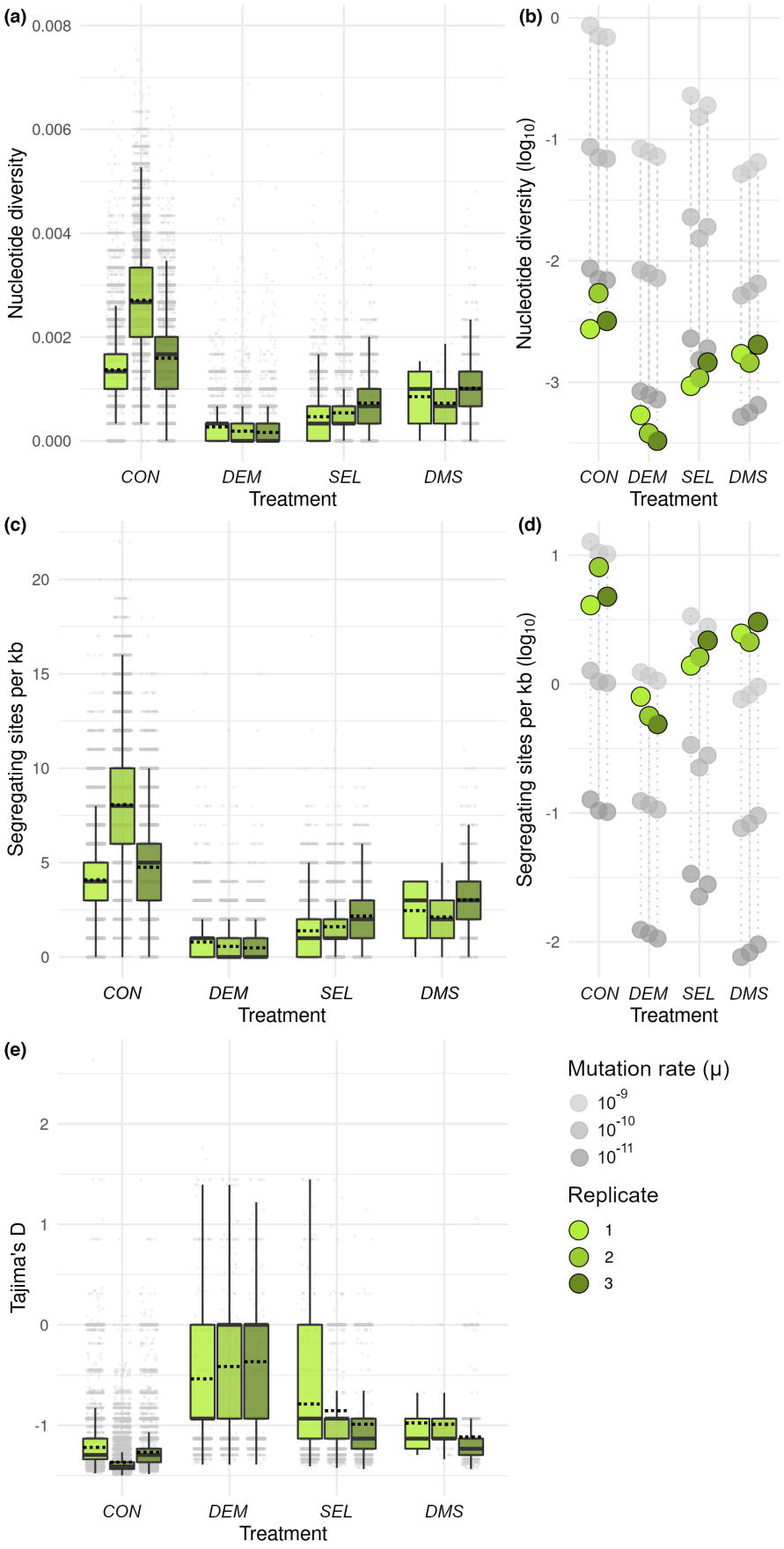

FIGURE 3 Observed and expected values of nucleotide diversity and segregating sites. (a) Observed nucleotide diversity in the algal populations. Points correspond to nucleotide diversity in genomic windows of 1 kb. Green boxplots contain half of the data points; a continuous line and a dotted line give median and mean values. (b) Green dots are mean observed values of nucleotide diversity. Grey dots mark expectations at three equilibria given by $2N_e\mu$, with three values of μ (10^{-9}, 10^{-10} and 10^{-11}) coloured with different shades of grey. Each population's value of N_e was approximated with the harmonic mean of daily population sizes. (c) Observed segregating sites per 1 kb. Boxplots contain half of the data points; a continuous and a dotted line mark the median and mean values. (d) Green dots are averaged empirical measures of segregating sites. Grey dots represent S_{exp} and were calculated with the formula given in the text. Results for three values of μ (10^{-9}, 10^{-10} and 10^{-11}) are presented with different grey shadings. N_e was approximated with the harmonic mean of population size. (e) Distribution of Tajima's *D* among genomic windows of 1 kb.

Retel et al., 2019). Periods of population size increase (days 20–30 and days 45–50) coincided with the spread of resistant host types, showing that the expansion of one or more resistant lineages drives population growth (Figures 1 and 2a). A general expectation is that bottlenecked populations experience more random effects through increased genetic drift and lower mutation supply than large populations of constant size (Garoff et al., 2020, Windels et al., 2021; but see Freitas et al., 2021). However, the high repeatability of the timing of population size fluctuations in treatment *DMS* was not observed in treatment *SEL* where demographic fluctuations were reduced and bottlenecks weaker (Figure 1). Generally, differences in dilution rate can affect the length of the periods in cyclical populations and the transient time, and can lead to complex population dynamics (Becks et al., 2005; Becks & Arndt, 2013; Fussmann et al., 2000).

Phenotypic change in the algae populations depended on the treatments they experienced. Resistance evolved only in the presence of virus. The evolution of resistance was faster in the treatment with little demographic fluctuations (*SEL*) than in the treatment with large fluctuations (*DMS*). This faster adaptation is in agreement with previous experiments that showed that bottlenecks and low population sizes can slow down adaptation (e.g., Windels et al., 2021, although see Izutsu et al., 2021). We further observed an increase in algal growth rate in the two treatments that maintained high population sizes, *CON* and *SEL* (Figure 2b). In the treatment *SEL* where the dilution rate was increased (0.3) compared to other treatments (0.1), we measured an increase in growth rate (+22% between days 0 and 60), which could be an adaptation to the increased death rate due to the increased number of algae that are washed out (e.g., Stearns et al., 2000). It is further possible that the evolution of a faster growth rate of the algae and/or the increased washout in treatment *SEL* results in a comparatively faster spread of resistance alleles in this treatment.

Our results demonstrate a strong negative effect on genetic diversity that was caused by large demographic fluctuations. When compared to control populations (*CON*), populations of treatment *DEM* had the strongest deficit of genetic diversity. This result adds to previous findings that population size can be a key driver of genetic diversity even in large populations typical in microorganisms and it is likely to constrain their adaptive potential (Garoff et al., 2020; Papkou et al., 2016, 2021; Windels et al., 2021). We likewise found that the selection exerted by viruses in treatment *SEL* lowered genetic diversity compared to *CON* populations. When comparing experimental measures with theoretical expectations that account for measured population sizes, we found that the diversity levels in treatment *SEL* and in treatment *DEM* are in a similar range to the diversity levels in treatment *CON*. This suggests that both nucleotide diversity and segregating sites in treatments *SEL*, *DEM* and *CON* are at comparable distances to their mutation–drift equilibria. The decreasing effect of selective sweeps in treatment *SEL* on genetic diversity thus appears to be weak or mitigated when compared with the effect of demography. The weak impact of selective sweeps in reducing genetic diversity is most striking when observing the host's genetic diversity in treatment *DMS*. Populations in treatment *DMS* consistently had higher nucleotide diversities and higher densities of segregating sites than those in treatment *DEM* and *SEL*. This relative excess remained when accounting for the respective population sizes of each culture (Figure 3). Our experiment suggests that the interaction of two different evolutionary scales, molecular and demographic, can affect the host's diversity positively and thereby favour adaptions to further viral strains (as discussed in Retel et al., 2019). The magnitude of this interaction suggests it can be an important factor in the co-evolution of *Chlorella* and PBCV-1. In a former experiment where temperature was used as a selective agent and where dilutions were used to induce bottlenecks in bacteria, interactions between selection and demography were found to affect genome-wide allele frequencies but did not impact nucleotide diversity (Wein & Dagan, 2019). Our experiment found contrary results, suggesting the need to investigate under which conditions an interaction emerges. Namely, it is unresolved whether a positive interaction on diversity is specific to host–parasite dynamics where the bottleneck follows a period of weak to no selection by the virus, or whether it extends to broader scenarios of selection with strong demographic fluctuations, as commonly encountered in response to abiotic stressors. Theoretical models will be helpful to find the conditions and factors that lead diversity to be positively affected by interacting demography and selection and may include competition for resources, trade-offs caused by resistance, and clonal interferences.

The positive effect of the interactions between selection and demographic fluctuations on genetic diversity that we measured in our experiment could emerge either through mechanisms that increase the supply of mutations, as well as mechanisms that facilitate the maintenance of segregating variation during sweeps and bottlenecks. Mutation supply increases when mutation rates increase, which has been observed in bacteria and yeast as a response to environmental change (Swings et al., 2017), or was selected for through prolonged successions of bottlenecks with selection (De Ste Croix et al., 2020). Evolution of the algae's mutation rates, however, is unlikely to happen as quickly and repeatedly to explain the consistent excess of diversity in all three replicates of the treatment *DMS* over a duration of only 60 days (~60 generations). Mutation supply can also increase through faster cell divisions, if resources increase or if a faster life cycle evolves. Increases in growth rates in our experiment evolved in treatments with large population sizes, *CON* and *SEL*, but not in *DMS*, the treatment with the increased diversity, indicating that growth rate evolution is unlikely to be the cause of the increased genetic diversity. Besides the supply of mutations, it is relevant to consider the probability and dynamics of de novo mutations establishing in populations. Previous studies have demonstrated that during neutral population expansion mutations accumulate following a simple power law (Kessler & Levine, 2013; Luria & Delbrück, 1943; Williams et al., 2016, 2018) and that this allows the rapid buildup of genetic diversity after selective sweeps (Retel et al., 2019). This mechanism might be particularly relevant in treatment *DMS* due to its dependence on both selection of a clonal lineage and its subsequent exponential growth, and matches the

previously observed frequency distribution of mutations during the sweep in treatment *DMS* (Retel et al., 2019).

Besides changes in mutation supply, interactions between demography and selection might facilitate the retention of segregating variants through bottleneck phases and sweeps. In an asexual system with a high-mutation regime (i.e., multiple resistant lineages compete for growth), theoretical studies have found that the feedback between demography and selection has an effect on allele fixation rates (Campos & Wahl, 2009). This feedback occurs through changes in the strength of genetic drift caused by population size variations that are compensated for by changes in the strength of clonal interferences. Furthermore, the retention of multiple lineages at intermediate frequencies could be facilitated if multiple resistance alleles participate in population regrowth (Chevin et al., 2008; Kim & Stephan, 2003; Stephan, 2019). Such a mechanism might favour genetic diversity in *DMS* if there are more interferences in *DMS* than in *SEL*. This could be the case if density-dependent effects caused by population size fluctuations affect the evolutionary dynamics of the treatments (Lopez Pascua et al., 2014). One indication that *SEL* and *DMS* have different evolutionary dynamics is that we observed resistance evolving at a slower pace in *DMS* compared to in *SEL*, and that the time intervals between maximum and minimum population sizes are longer in *DMS* compared to *SEL* populations. A comparatively slower speed of co-evolution, through the slower turnover of host strains, would facilitate the accumulation of mutations and increase genetic diversity, a pattern that matches our observations.

Recent experimental and theoretical studies reveal how interactions of selective regimes and demographic fluctuations can lead to interesting, sometimes counterintuitive outcomes (e.g., Izutsu et al., 2021; Mahrt et al., 2021). Our experiment provides measures of the role of selection, demography and their interaction as they occur throughout early host–parasite co-evolution. We found that both selection and demographic fluctuations have a negative effect on genetic diversity. Most interestingly, we observed that the combination of demographic fluctuations with the selection exerted by the virus largely dampened the loss of genetic diversity compared to populations that experienced either fluctuations or selection. Our results suggest that, in this algae–virus system, genetic diversity is not explained only by mutation, drift, or by selective sweeps for resistance alleles, but other factors that emerge from a demography–selection interaction play a considerable role. Our results experimentally demonstrate that populations experiencing a combination of selective and demographic constraints accumulate more genetic diversity than expected a priori from their demographic history, and that this interaction allows host populations to retain potential for further adaptations.

AUTHOR CONTRIBUTIONS

Lutz Becks and Philine G. D. Feulner conceived and designed the study. Vienna Kowallik carried out the experiment. Guénolé Le Pennec and Cas Retel processed the sequence data, performed statistics and produced visuals. Guénolé Le Pennec, Cas Retel, Lutz Becks and Philine G. D. Feulner interpreted the results. Guénolé Le Pennec wrote the manuscript. All the authors reviewed the manuscript.

ACKNOWLEDGEMENTS

We are grateful to the teams at the MPI sequencing centre in Plön and at the NGS platform at Bern University (VetSuisse) for carrying out the DNA sequencing, and to G. Bartolomucci for help with collection of the phenotypic data. Genomic data analysis was supported by collaboration with the Genetic Diversity Centre (GDC), ETH Zürich. We would like to thank the reviewers who helped to improve the manuscript, members of the SPP1819 for their advice throughout the project, as well as the Fish Genomics research group in Kastanienbaum for helpful comments on a previous version of the manuscript. Funding was provided by the German Research Foundation (DFG) to L.B. (grants BE 4135/5 and 4135/9) and by the Swiss National Science Foundation (SNSF) to P.G.D.F. (grants 310030E-160812 and 310030E_179637) within the DFG Priority Program SPP1819. Open access funding provided by ETH-Bereich Forschungsanstalten.

CONFLICT OF INTEREST

The authors declare no conflicts of interest.

DATA AVAILABILITY STATEMENT

Population size data, phenotypic data and data tables with nucleotide diversity are available in the Supplementary Information and are also deposited on the EAWAG research data institutional collections (https://doi.org/10.25678/0007HK). Bash scripts for the processing of sequence data and R scripts to perform other analyses and to reproduce the manuscript's figures are available on the EAWAG research data institutional collections (https://doi.org/10.25678/0007HK). All associated raw sequencing data have been deposited in the European Nucleotide Archive (Accession no. PRJEB56525).

ORCID

Lutz Becks https://orcid.org/0000-0002-3885-5253
Philine G. D. Feulner https://orcid.org/0000-0002-8078-1788

REFERENCES

Abdul-Rahman, F., Tranchina, D., & Gresham, D. (2021). Fluctuating environments maintain genetic diversity through neutral fitness effects and balancing selection. *Molecular Biology and Evolution*, *38*(10), 4362–4375. https://doi.org/10.1093/molbev/msab173

Agarkova, I., Hertel, B., Zhang, X., Lane, L., Tchourbanov, A., Dunigan, D. D., Thiel, G., Rossmann, M. G., & Van Etten, J. L. (2014). Dynamic attachment of Chlorovirus PBCV-1 to *Chlorella variabilis*. *Virology*, *466–467*, 95–102. https://doi.org/10.1016/j.virol.2014.07.002

Aguadé, M., Meyers, W., Long, A. D., & Langley, C. H. (1994). Single-strand conformation polymorphism analysis coupled with stratified DNA sequencing reveals reduced sequence variation in the su(s) and su(wa) regions of the *Drosophila melanogaster* X chromosome. *Proceedings of the National Academy of Sciences of the United States of America*, *91*(11), 4658–4662.

Antonio-Nkondjio, C., Sonhafouo-Chiana, N., Ngadjeu, C. S., Doumbe-Belisse, P., Talipouo, A., Djonkam, D., Kopya, E., Bamou, R., Awono-Ambene, P., & Wondji, C. S. (2017). Review of the evolution

of insecticide resistance in main malaria vectors in Cameroon from 1990 to 2017. *Parasites & Vectors*, *10*(1), 472. https://doi.org/10.1186/s13071-017-2417-9

Ashby, B., Iritani, R., Best, A., White, A., & Boots, M. (2019). Understanding the role of eco-evolutionary feedbacks in host-parasite coevolution. *Journal of Theoretical Biology*, *464*, 115–125. https://doi.org/10.1016/j.jtbi.2018.12.031

Barrett, R. D. H., & Schluter, D. (2008). Adaptation from standing genetic variation. *Trends in Ecology & Evolution*, *23*(1), 38–44. https://doi.org/10.1016/j.tree.2007.09.008

Bartoń, K. (2022). *MuMIn: Multi-Model Inference*. *R package version 1.46.0*. https://CRAN.R-project.org/package=MuMIn

Bates, D., Mächler, M., Bolker, B., & Walker, S. (2015). Fitting linear mixed-effects models using Lme4. *Journal of Statistical Software*, *67*, 1–48. https://doi.org/10.18637/jss.v067.i01

Becks, L., & Arndt, H. (2013). Different types of synchrony in chaotic and cyclic communities. *Nature Communications*, *4*(1), 1359. https://doi.org/10.1038/ncomms2355

Becks, L., Hilker, F. M., Malchow, H., Jürgens, K., & Arndt, H. (2005). Experimental demonstration of chaos in a microbial food web. *Nature*, *435*(7046), 1226–1229. https://doi.org/10.1038/nature03627

Begun, D. J., & Aquadro, C. F. (1992). Levels of naturally occurring DNA polymorphism correlate with recombination rates in *D. melanogaster*. *Nature*, *356*(6369), 519–520. https://doi.org/10.1038/356519a0

Bell, G. (2013). Evolutionary rescue and the limits of adaptation. *Philosophical Transactions of the Royal Society B: Biological Sciences*, *368*(1610), 20120080. https://doi.org/10.1098/rstb.2012.0080

Bitter, M. C., Kapsenberg, L., Gattuso, J.-P., & Pfister, C. A. (2019). Standing genetic variation fuels rapid adaptation to ocean acidification. *Nature Communications*, *10*(1), 5821. https://doi.org/10.1038/s41467-019-13767-1

Blanc, G., Duncan, G., Agarkova, I., Borodovsky, M., Gurnon, J., Kuo, A., Lindquist, E., Lucas, S., Pangilinan, J., Polle, J., Salamov, A., Terry, A., Yamada, T., DD Dunigan, G., IV, Claverie, J.-M., & Van Etten, J. L. (2010). The *Chlorella variabilis* NC64A genome reveals adaptation to photosymbiosis, coevolution with viruses, and cryptic sex. *The Plant Cell*, *22*(9), 2943–2955. https://doi.org/10.1105/tpc.110.076406

Brockhurst, M. A., Morgan, A. D., Fenton, A., & Buckling, A. (2007). Experimental coevolution with bacteria and phage. The *Pseudomonas fluorescens*—Φ2 model system. *Infection, Genetics and Evolution*, *7*(4), 547–552. https://doi.org/10.1016/j.meegid.2007.01.005

Buckingham, L. J., & Ashby, B. (2022). Coevolutionary theory of hosts and parasites. *Journal of Evolutionary Biology*, *35*(2), 205–224. https://doi.org/10.1111/jeb.13981

Buckling, A., & Brockhurst, M. (2012). Bacteria-virus coevolution. *Advances in Experimental Medicine and Biology*, *751*, 347–370. https://doi.org/10.1007/978-1-4614-3567-9_16

Buffalo, V. (2021). Quantifying the relationship between genetic diversity and population size suggests natural selection cannot explain Lewontin's paradox. *eLife*, *10*, e67509. https://doi.org/10.7554/eLife.67509

Calla, B., Demkovich, M., Siegel, J. P., Viana, J. P. G., Walden, K. K. O., Robertson, H. M., & Berenbaum, M. R. (2021). Selective sweeps in a nutshell: The genomic footprint of rapid insecticide resistance evolution in the almond agroecosystem. *Genome Biology and Evolution*, *13*(1), evaa234. https://doi.org/10.1093/gbe/evaa234

Campos, P. R. A., & Wahl, L. M. (2009). The effects of population bottlenecks on clonal interference, and the adaptation effective population size. *Evolution*, *63*(4), 950–958. https://doi.org/10.1111/j.1558-5646.2008.00595.x

Charlesworth, B. (2020). How good are predictions of the effects of selective sweeps on levels of neutral diversity? *Genetics*, *216*(4), 1217–1238. https://doi.org/10.1534/genetics.120.303734

Chen, S., Zhou, Y., Chen, Y., & Gu, J. (2018). Fastp: An ultra-fast all-in-one FASTQ preprocessor. *Bioinformatics*, *34*(17), i884–i890. https://doi.org/10.1093/bioinformatics/bty560

Chevin, L.-M., Billiard, S., & Hospital, F. (2008). Hitchhiking both ways: Effect of two interfering selective sweeps on linked neutral variation. *Genetics*, *180*(1), 301–316. https://doi.org/10.1534/genetics.108.089706

Corbett-Detig, R. B., Hartl, D. L., & Sackton, T. B. (2015). Natural selection constrains neutral diversity across a wide range of species. *PLoS Biology*, *13*(4), e1002112. https://doi.org/10.1371/journal.pbio.1002112

Cvijović, I., Good, B. H., & Desai, M. M. (2018). The effect of strong purifying selection on genetic diversity. *Genetics*, *209*(4), 1235–1278. https://doi.org/10.1534/genetics.118.301058

de Andreazzi, C. S., Guimarães, P. R., & Melián, C. J. (2018). Eco-evolutionary feedbacks promote fluctuating selection and long-term stability of antagonistic networks. *Proceedings of the Royal Society B: Biological Sciences*, *285*(1874), 20172596. https://doi.org/10.1098/rspb.2017.2596

De Ste Croix, M., Holmes, J., Wanford, J. J., Moxon, E. R., Oggioni, M. R., & Bayliss, C. D. (2020). Selective and non-selective bottlenecks as drivers of the evolution of hypermutable bacterial loci. *Molecular Microbiology*, *113*(3), 672–681. https://doi.org/10.1111/mmi.14453

Ekroth, A. K. E., Rafaluk-Mohr, C., & King, K. C. (2019). Host genetic diversity limits parasite success beyond agricultural systems: A meta-analysis. *Proceedings of the Royal Society B: Biological Sciences*, *286*(1911), 20191811. https://doi.org/10.1098/rspb.2019.1811

Ellegren, H., & Galtier, N. (2016). Determinants of genetic diversity. *Nature Reviews. Genetics*, *17*(7), 422–433. https://doi.org/10.1038/nrg.2016.58

Freitas, O., Wahl, L. M., & Campos, P. R. A. (2021). Robustness and predictability of evolution in bottlenecked populations. *Physical Review E*, *103*(4), 042415. https://doi.org/10.1103/PhysRevE.103.042415

Frickel, J., Feulner, P. G. D., Karakoc, E., & Becks, L. (2018). Population size changes and selection drive patterns of parallel evolution in a host–virus system. *Nature Communications*, *9*(1), 1706. https://doi.org/10.1038/s41467-018-03990-7

Frickel, J., Sieber, M., & Becks, L. (2016). Eco-evolutionary dynamics in a coevolving host–virus system. *Ecology Letters*, *19*(4), 450–459. https://doi.org/10.1111/ele.12580

Fussmann, G. F., Ellner, S. P., Shertzer, K. W., & Hairston, N. G., Jr. (2000). Crossing the hopf bifurcation in a live predator-prey system. *Science*, *290*(5495), 1358–1360. https://doi.org/10.1126/science.290.5495.1358

Garoff, L., Pietsch, F., Huseby, D. L., Lilja, T., Brandis, G., & Hughes, D. (2020). Population bottlenecks strongly influence the evolutionary trajectory to fluoroquinolone resistance in *Escherichia coli*. *Molecular Biology and Evolution*, *37*(6), 1637–1646. https://doi.org/10.1093/molbev/msaa032

Gokhale, C. S., Papkou, A., Traulsen, A., & Schulenburg, H. (2013). Lotka–Volterra dynamics kills the red queen: Population size fluctuations and associated stochasticity dramatically change host-parasite coevolution. *BMC Evolutionary Biology*, *13*(1), 254. https://doi.org/10.1186/1471-2148-13-254

Hairston, N. G., Jr., Ellner, S. P., Geber, M. A., Yoshida, T., & Fox, J. A. (2005). Rapid evolution and the convergence of ecological and evolutionary time. *Ecology Letters*, *8*(10), 1114–1127. https://doi.org/10.1111/j.1461-0248.2005.00812.x

Hartl, D. L., & Clark, A. G. (2007). *Principles of population genetics* (4th ed.). Oxford University Press.

Hendry, A. P., & Kinnison, M. T. (1999). Perspective: The pace of modern life: Measuring rates of contemporary microevolution. *Evolution*, *53*(6), 1637–1653. https://doi.org/10.2307/2640428

Hesse, E., & Buckling, A. (2016). Host population bottlenecks drive parasite extinction during antagonistic coevolution. *Evolution*, *70*(1), 235–240. https://doi.org/10.1111/evo.12837

Izutsu, M., Lake, D. M., Matson, Z. W. D., Dodson, J. P., & Lenski, R. E. (2021). Effects of periodic bottlenecks on the dynamics of adaptive evolution in microbial populations. *bioRxiv*. https://doi.org/10.1101/2021.12.29.474457

Kessler, D. A., & Levine, H. (2013). Large population solution of the stochastic Luria–Delbrück evolution model. *Proceedings of the National Academy of Sciences of the United States of America*, *110*(29), 11682–11687. https://doi.org/10.1073/pnas.1309667110

Kim, Y., & Stephan, W. (2003). Selective sweeps in the presence of interference among partially linked loci. *Genetics*, *164*(1), 389–398. https://doi.org/10.1093/genetics/164.1.389

Kirchner, J. (2020). Data analysis toolkits. *EnviDat*. https://doi.org/10.16904/envidat.177

Kofler, R., Orozco-terWengel, P., Maio, N. D., Pandey, R. V., Nolte, V., Futschik, A., Kosiol, C., & Schlötterer, C. (2011). PoPoolation: A toolbox for population genetic analysis of next generation sequencing data from pooled individuals. *PLoS One*, *6*(1), e15925. https://doi.org/10.1371/journal.pone.0015925

Leffler, E. M., Bullaughey, K., Matute, D. R., Meyer, W. K., Ségurel, L., Venkat, A., Andolfatto, P., & Przeworski, M. (2012). Revisiting an old riddle: What determines genetic diversity levels within species? *PLoS Biology*, *10*(9), e1001388. https://doi.org/10.1371/journal.pbio.1001388

Li, H., & Durbin, R. (2009). Fast and accurate short read alignment with burrows-wheeler transform. *Bioinformatics*, *25*(14), 1754–1760. https://doi.org/10.1093/bioinformatics/btp324

Li, H., Handsaker, B., Wysoker, A., Fennell, T., Ruan, J., Homer, N., Marth, G., Abecasis, G., Durbin, R., & 1000 Genome Project Data Processing Subgroup. (2009). The sequence alignment/map format and SAMtools. *Bioinformatics*, *25*(16), 2078–2079. https://doi.org/10.1093/bioinformatics/btp352

Lopez Pascua, L., Hall, A. R., Best, A., Morgan, A. D., Boots, M., & Buckling, A. (2014). Higher resources decrease fluctuating selection during host-parasite coevolution. *Ecology Letters*, *17*(11), 1380–1388. https://doi.org/10.1111/ele.12337

Luria, S. E., & Delbrück, M. (1943). Mutations of bacteria from virus sensitivity to virus resistance. *Genetics*, *28*(6), 491–511. https://doi.org/10.1093/genetics/28.6.491

Mahrt, N., Tietze, A., Künzel, S., Franzenburg, S., Barbosa, C., Jansen, G., & Schulenburg, H. (2021). Bottleneck size and selection level reproducibly impact evolution of antibiotic resistance. *Nature Ecology & Evolution*, *5*(9), 1233–1242. https://doi.org/10.1038/s41559-021-01511-2

Maynard Smith, J., & Haigh, J. (1974). The hitch-hiking effect of a favourable gene. *Genetical Research*, *23*(1), 23–35.

Messer, P. W., Ellner, S. P., & Hairston, N. G. (2016). Can population genetics adapt to rapid evolution? *Trends in Genetics*, *32*(7), 408–418. https://doi.org/10.1016/j.tig.2016.04.005

Miller, M. P., & Vincent, E. R. (2008). Rapid natural selection for resistance to an introduced parasite of rainbow trout. *Evolutionary Applications*, *1*(2), 336–341.

Mizoguchi, K., Morita, M., Fischer, C. R., Yoichi, M., Tanji, Y., & Unno, H. (2003). Coevolution of bacteriophage PP01 and *Escherichia coli* O157:H7 in continuous culture. *Applied and Environmental Microbiology*, *69*(1), 170–176. https://doi.org/10.1128/AEM.69.1.170-176.2003

Nakagawa, S., Johnson, P. C. D., & Schielzeth, H. (2017). The coefficient of determination R2 and intra-class correlation coefficient from generalized linear mixed-effects models revisited and expanded. *Journal of the Royal Society Interface*, *14*(134), 20170213. https://doi.org/10.1098/rsif.2017.0213

Nei, M., Maruyama, T., & Chakraborty, R. (1975). The bottleneck effect and genetic variability in populations. *Evolution*, *29*(1), 1–10. https://doi.org/10.2307/2407137

Osmond, M. M., & Coop, G. (2020). Genetic signatures of evolutionary rescue by a selective sweep. *Genetics*, *215*(3), 813–829. https://doi.org/10.1534/genetics.120.303173

Papkou, A., Gokhale, C. S., Traulsen, A., & Schulenburg, H. (2016). Host–parasite coevolution: Why changing population size matters. *Zoology, SI: Host-Parasite Coevolution*, *119*(4), 330–338. https://doi.org/10.1016/j.zool.2016.02.001

Papkou, A., Schalkowski, R., Barg, M.-C., Koepper, S., & Schulenburg, H. (2021). Population size impacts host–pathogen coevolution. *Proceedings of the Royal Society B: Biological Sciences*, *288*(1965), 20212269. https://doi.org/10.1098/rspb.2021.2269

R Core Team. (2022). *R: A language and environment for statistical computing*. R Foundation for Statistical Computing. https://www.R-project.org/

Retel, C., Kowallik, V., Becks, L., & Feulner, P. G. D. (2022). Strong selection and high mutation supply characterize experimental Chlorovirus evolution. *Virus Evolution*, *8*, veac003. https://doi.org/10.1093/ve/veac003

Retel, C., Kowallik, V., Huang, W., Werner, B., Künzel, S., Becks, L., & Feulner, P. G. D. (2019). The feedback between selection and demography shapes genomic diversity during coevolution. *Science Advances*, *5*(10), eaax0530. https://doi.org/10.1126/sciadv.aax0530

Rice, S. H. (2004). *Evolutionary theory, mathematical and conceptual foundations* (1st ed.). Oxford University Press.

Schulte, R. D., Makus, C., Hasert, B., Michiels, N. K., & Schulenburg, H. (2010). Multiple reciprocal adaptations and rapid genetic change upon experimental coevolution of an animal host and its microbial parasite. *Proceedings of the National Academy of Sciences of the United States of America*, *107*(16), 7359–7364. https://doi.org/10.1073/pnas.1003113107

Stearns, S. C., Ackermann, M., Doebeli, M., & Kaiser, M. (2000). Experimental evolution of aging, growth, and reproduction in fruitflies. *Proceedings of the National Academy of Sciences of the United States of America*, *97*(7), 3309–3313. https://doi.org/10.1073/pnas.97.7.3309

Stephan, W. (2019). Selective sweeps. *Genetics*, *211*(1), 5–13. https://doi.org/10.1534/genetics.118.301319

Stern, A., & Sorek, R. (2011). The phage-host arms-race: Shaping the evolution of microbes. *BioEssays*, *33*(1), 43–51. https://doi.org/10.1002/bies.201000071

Swings, T., Bergh, B. v. d., Wuyts, S., Oeyen, E., Voordeckers, K., Verstrepen, K. J., Fauvart, M., Verstraeten, N., & Michiels, J. (2017). Adaptive tuning of mutation rates allows fast response to lethal stress in *Escherichia coli*. *eLife*, *6*, e22939. https://doi.org/10.7554/eLife.22939

Tajima, F. (1989). The effect of change in population size on DNA polymorphism. *Genetics*, *123*(3), 597–601.

van Velzen, E., & Gaedke, U. (2017). Disentangling eco-evolutionary dynamics of predator-prey coevolution: The case of antiphase cycles. *Scientific Reports*, *7*(1), 17125. https://doi.org/10.1038/s41598-017-17019-4

van Velzen, E., & Gaedke, U. (2018). Reversed predator–prey cycles are driven by the amplitude of prey oscillations. *Ecology and Evolution*, *8*(12), 6317–6329. https://doi.org/10.1002/ece3.4184

Waclaw, B. (2016). Evolution of drug resistance in bacteria. *Advances in Experimental Medicine and Biology*, *915*, 49–67. https://doi.org/10.1007/978-3-319-32189-9_5

Watterson, G. A. (1975). On the number of segregating sites in genetical models without recombination. *Theoretical Population Biology*, *7*(2), 256–276. https://doi.org/10.1016/0040-5809(75)90020-9

Wein, T., & Dagan, T. (2019). The effect of population bottleneck size and selective regime on genetic diversity and evolvability in bacteria. *Genome Biology and Evolution*, *11*(1), 3283–3290. https://doi.org/10.1093/gbe/evz243

Williams, M. J., Werner, B., Barnes, C. P., Graham, T. A., & Sottoriva, A. (2016). Identification of neutral tumor evolution across cancer

types. *Nature Genetics*, *48*(3), 238–244. https://doi.org/10.1038/ng.3489

Williams, M. J., Werner, B., Heide, T., Curtis, C., Barnes, C. P., Sottoriva, A., & Graham, T. A. (2018). Quantification of subclonal selection in cancer from bulk sequencing data. *Nature Genetics*, *50*(6), 895–903. https://doi.org/10.1038/s41588-018-0128-6

Windels, E. M., Fox, R., Yerramsetty, K., Krouse, K., Wenseleers, T., Swinnen, J., Matthay, P., Verstraete, L., Wilmaerts, D., Van den Bergh, B., & Michiels, J. (2021). Population bottlenecks strongly affect the evolutionary dynamics of antibiotic persistence. *Molecular Biology and Evolution*, *38*(8), 3345–3357. https://doi.org/10.1093/molbev/msab107

Zuk, M., Rotenberry, J. T., & Tinghitella, R. M. (2006). Silent night: Adaptive disappearance of a sexual signal in a parasitized population of field crickets. *Biology Letters*, *2*(4), 521–524. https://doi.org/10.1098/rsbl.2006.0539

SUPPORTING INFORMATION

Additional supporting information can be found online in the Supporting Information section at the end of this article.

How to cite this article: Le Pennec, G., Retel, C., Kowallik, V., Becks, L., & Feulner, P. G. D. (2023). Demographic fluctuations and selection during host–parasite co-evolution interactively increase genetic diversity. *Molecular Ecology*, *00*, 1–14. https://doi.org/10.1111/mec.16939